

Impact of the inherent separation of scales in the Navier–Stokes- $\alpha\beta$ equations

Tae-Yeon Kim,¹ Massimo Cassiani,² John D. Albertson,² John E. Dolbow,² Eliot Fried,¹ and Morton E. Gurtin³

¹*Department of Mechanical Engineering, McGill University, Montréal, Québec, Canada H3A 2K6*

²*Department of Civil and Environmental Engineering, Duke University, Durham, North Carolina 27708, USA*

³*Department of Mathematical Sciences, Carnegie Mellon University, Pittsburgh, Pennsylvania 15213, USA*

(Received 31 October 2008; revised manuscript received 23 March 2009; published 28 April 2009)

We study the effect of the length scales α and β in the Navier–Stokes- $\alpha\beta$ equations on the energy spectrum and the alignment between the vorticity and the eigenvectors of the stretching tensor in three-dimensional homogeneous and isotropic turbulent flows in a periodic cubic domain, including the limiting cases of the Navier–Stokes- α and Navier–Stokes equations. A significant increase in the accuracy of the energy spectrum at large wave numbers arises for $\beta < \alpha$. The vorticity structures predicted by the Navier–Stokes- $\alpha\beta$ equations also improve as β decreases away from α . However, optimal choices for α and β depend not only on the problem of interest but also on the grid resolution.

DOI: 10.1103/PhysRevE.79.045307

PACS number(s): 47.27.ek, 47.27.Gs

Subgrid models for turbulence seek to capture the influence of small-scale motions on large-scale phenomena, allowing for accurate and efficient simulations of high-Reynolds-number flows while resolving only large-scale flow structures. The Navier–Stokes- α (NS- α) equations, which combine Lagrangian-averaged dispersive nonlinearity with Newtonian viscosity, provide one such model. These equations involve a parameter $\alpha > 0$, with dimensions of length, and direct numerical simulation (DNS) shows that they capture the properties of flows involving eddy scales greater than α [1]. Foias *et al.* [2] investigated the scaling properties of the energy spectrum for the NS- α equations. Graham *et al.* [3,4] studied numerically two-dimensional magnetohydrodynamic turbulence using the Lagrangian-averaged magnetohydrodynamic equations and investigated the NS- α equations at significantly high Reynolds numbers. The NS- α equations have also been compared to other related regularizations such as the Clark- α and Leray- α equations [5]. We examine a recent generalization, the Navier–Stokes- $\alpha\beta$ (NS- $\alpha\beta$) equations, that attempts to extend the applicability of the NS- α equations by accounting for the inherent separation of scales between the inertial and dissipation ranges.

Chen *et al.* [6–8] obtained the NS- α equations by adding a viscous term to the Euler- α equations of Holm *et al.* [9,10]. For a statistically homogeneous and isotropic turbulent flow of a fluid with constant density ρ and constant kinematic viscosity ν , the NS- α equations constitute a system

$$\frac{\partial \mathbf{v}}{\partial t} + (\text{grad } \mathbf{v})\mathbf{u} + (\text{grad } \mathbf{u})^T \mathbf{v} = -\text{grad} \frac{p}{\rho} + \nu \Delta \mathbf{v},$$

$$\mathbf{v} = (1 - \alpha^2 \Delta)\mathbf{u}, \quad \text{div } \mathbf{u} = 0, \quad (1)$$

for unfiltered and filtered velocities \mathbf{v} and \mathbf{u} and a filtered pressure p . In the context of Lagrangian averaging, α is the statistical correlation length of the excursion taken by a fluid particle away from its phase-averaged trajectory. More naively, α can be interpreted as the characteristic linear dimension of the smallest eddy resolvable by the model. Importantly, the NS equations are recovered from Eq. (1) in the null-filtering limit $\alpha \rightarrow 0$.

Working from a general framework for fluid-dynamical theories involving gradient dependencies [11], Fried and Gurtin derived a slight generalization [12,13],

$$\frac{\partial \mathbf{v}}{\partial t} + (\text{grad } \mathbf{v})\mathbf{u} + (\text{grad } \mathbf{u})^T \mathbf{v} = -\text{grad} \frac{p}{\rho} + \nu(1 - \beta^2 \Delta)\Delta \mathbf{u}, \quad (2)$$

of Eq. (1)₁; together, Eq. (1)_{2,3} and Eq. (2) are the NS- $\alpha\beta$ equations. Like α , $\beta > 0$ has dimensions of length. When Eq. (1)₂ is used to eliminate \mathbf{v} from Eq. (2), a regularized NS equation for \mathbf{u} results. This equation contains a dispersive term, of energetic origin, with coefficient α and a dissipative term with coefficient β . Within the phenomenological description of turbulence, it seems reasonable to view α as representative of eddy scales in the inertial range, where the dissipationless transfer of kinetic energy between intermediate scale eddies occurs, and β as representative of eddy scales in the dissipation range, where viscous damping converts the kinetic energy contained in the smallest eddies into heat [12,13]. One thus expects that $\beta < \alpha$. Since specializing Eq. (2) to Eq. (1)₁ entails setting β to α , the NS- α equations seem to involve an implicit equating of disparate length scales. This is a vestige of the conventional argument leading to Eq. (1), an argument which associates viscosity with the stretching tensor for the unfiltered velocity.

In this Rapid Communication, DNS is used to show that, consistent with the foregoing considerations, taking $\beta < \alpha$ in the NS- $\alpha\beta$ equations provides a means to capture the properties of flows involving eddy scales approaching β .

To begin, we use the identity $\text{grad}(\mathbf{u} \cdot \mathbf{v}) = (\text{grad } \mathbf{v})\mathbf{u} + (\text{grad } \mathbf{u})^T \mathbf{v} + \mathbf{u} \times \mathbf{q}$, with $\mathbf{q} = \text{curl } \mathbf{v}$, to rewrite Eq. (2) as

$$\frac{\partial \mathbf{v}}{\partial t} + (\text{grad } \mathbf{u})\mathbf{v} - \mathbf{u} \times \mathbf{q} = -\text{grad} \frac{p}{\rho} + \nu(1 - \beta^2 \Delta)\Delta \mathbf{u}. \quad (3)$$

By Eq. (1)_{2,3}, the unfiltered velocity \mathbf{v} is solenoidal,

$$\text{div } \mathbf{v} = 0. \quad (4)$$

Moreover, Eqs. (1)₂ and (4) imply Eq. (1)₃. With the identification $\mathbf{q} = \text{curl } \mathbf{v}$, the system comprised by Eqs. (1)_{2,3} and (2) is thus equivalent to that comprised by Eqs. (1)₂, (3) and (4).

Approximating the unfiltered velocity \mathbf{v} by a finite collec-

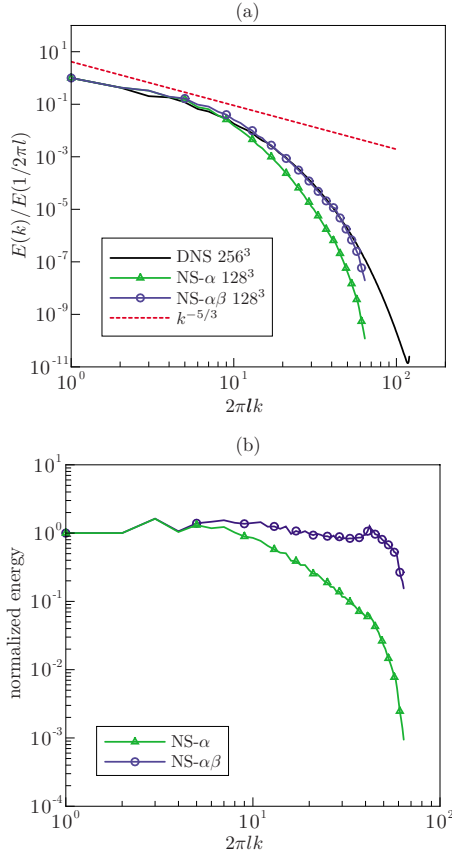


FIG. 1. (Color online) (a) Energy spectra for NS, NS- α ($\alpha = \pi/4$), and NS- $\alpha\beta$ ($\alpha = \pi/4$ and $\beta = \pi/6$). (b) Energy spectra for the NS- α and NS- $\alpha\beta$ results of (a) normalized by the energy spectrum for NS of (a).

tion \mathcal{I} of Fourier modes $\mathbf{v}_{\mathbf{k}}$ via $\mathbf{v}(\mathbf{x}, t) = \sum_{\mathcal{I}} \mathbf{v}_{\mathbf{k}}(t) e^{i\mathbf{k}\cdot\mathbf{x}}$ and substituting into Eqs. (1)₂, (3) and (4), we obtain pseudospectral equations of the form

$$\frac{d\mathbf{v}_{\mathbf{k}}}{dt} = \mathbf{P}_{\mathbf{k}}(\mathbf{u} \times \mathbf{q})_{\mathbf{k}} - \nu \frac{1 + k^2 \beta^2}{1 + k^2 \alpha^2} k^2 \mathbf{v}_{\mathbf{k}} + \mathbf{f}_{\mathbf{k}},$$

$$\mathbf{v}_{\mathbf{k}} = (1 + \alpha^2 k^2) \mathbf{u}_{\mathbf{k}}, \quad \mathbf{k} \cdot \mathbf{v}_{\mathbf{k}} = 0, \quad (5)$$

where $\mathbf{P}_{\mathbf{k}} = \mathbf{1} - \mathbf{k} \otimes \mathbf{k} / |\mathbf{k}|^2$ is the spectral projection operator, $k = |\mathbf{k}|$ is the wave number, and the forcing term $\mathbf{f}_{\mathbf{k}}$ is introduced to ensure that the total energy contained in each of the first two wave-number shells remain constant in time with ratio consistent with Kolmogorov's $-5/3$ law [1]. Setting β to α in Eq. (5)₁ gives Eq. (37) of Chen *et al.* [1].

The pseudospectral equations were discretized using full de-aliasing and second-order Adams-Bashforth time stepping. The code is based on one discussed by Albertson and Parlange [14,15]. A cubic flow domain with side-length $2\pi l$ and periodic boundary conditions was considered. To enforce periodicity, \mathcal{I} was restricted suitably. The initial velocity was taken to be a Gaussian with prescribed energy spectrum proportional to $k^4 \exp[-2(k/k_0)^2]$, with $k_0 l = 5$.

Flow statistics were calculated by averaging over several large-eddy turnover times $2\pi l / u'$, where the mean velocity fluctuation u' is given via the energy spectrum $E(k)$ by u'

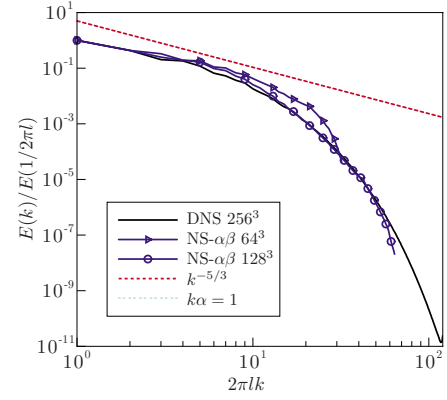


FIG. 2. (Color online) Comparison of the NS- $\alpha\beta$ equation at lower resolutions with the NS-equation simulation at higher resolution.

$= [2 \int_0^\infty E(k) dk / 3]^{1/2}$. To present dimensionless results, we write $E(1/2\pi l)$ for the energy in the first two shells and define a characteristic time $\tau = l / \sqrt{5E(1/2\pi l)} / 6$ associated with the forcing $\mathbf{f}_{\mathbf{k}}$. All results reported are for intervals no shorter than one required for five large-eddy turnovers.

Figure 1 shows normalized energy spectra obtained using a resolution of 128^3 and a normalized kinematic viscosity of $\nu\tau/l^2 = 0.01$. Plots are provided for three choices of α and β : $\alpha = \beta = 0$ (NS); $\alpha = \pi/4$ and $\beta = \alpha$ (NS- α); and $\alpha = \pi/4$ and $\beta = \pi/6$ (NS- $\alpha\beta$). The corresponding computed values of the Taylor microscale Reynolds number R_λ are all similar: 52 (NS), 58 (NS- α), and 51 (NS- $\alpha\beta$). The results for NS- α are close to those reported by Chen *et al.* [1]. Although the NS- α results follow Kolmogorov's $-5/3$ law in the inertial range, they do not agree with the NS results for $k\alpha > 1$. However, the NS- $\alpha\beta$ and NS results are indistinguishable in both the inertial and dissipation ranges. These results are consistent with the realization that setting β to α overdamps the response and that setting $\beta < \alpha$ allows for a greater portion of the inertial range to be captured. Although no effort was made to optimize the choice of β for the selected value $\pi/4$ of α , choosing $\beta = \pi/6$ allows recovery of an additional decade of the energy spectrum. Other choices of β might well yield further improvements.

Figure 1 also shows the NS- α and NS- $\alpha\beta$ energy spectra of Fig. 1 normalized by the energy spectrum obtained from the NS equations at each wave number. These curves accentuate the improved accuracy of the NS- $\alpha\beta$ results, particularly for $k\alpha > 1$. The normalized NS- $\alpha\beta$ results are closer to unity over a much greater interval of wave numbers, only predicting a slight overshoot at low ($1 \leq 2\pi lk \leq 10$) and high ($40 \leq 2\pi lk \leq 45$) wave numbers. This discrepancy, which is most pronounced at low wave numbers, is also exhibited by the NS- α model and might be partially due to the use of a forcing scheme designed for the NS equations [16]. Finally, while the NS- $\alpha\beta$ spectrum begins to diverge from that arising from the NS equations at wave numbers $2\pi lk > 45$, it is nonetheless two orders of magnitude more accurate than the counterpart arising from the NS- α equations.

The overshoot generated by the NS- $\alpha\beta$ equations for $k\alpha > 1$ seems to depend on the choice of β and the resolution. Figure 2 shows the normalized energy spectrum for resolu-

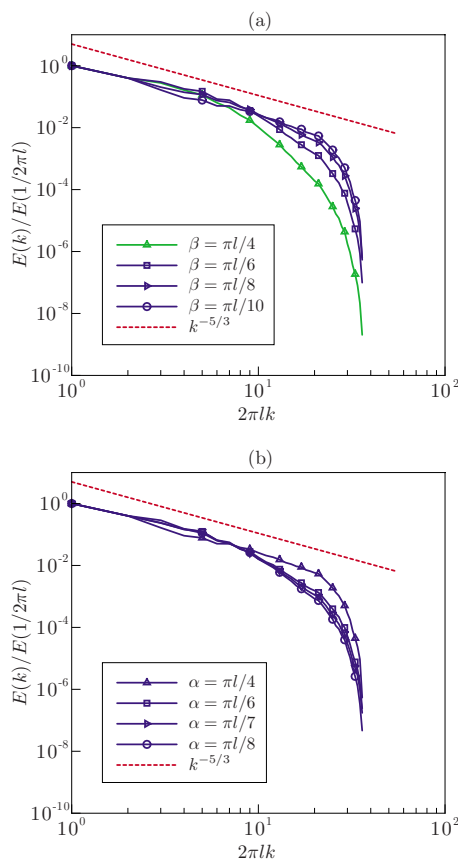


FIG. 3. (Color online) Influence, 64^3 resolution, of (a) β with $\alpha = \pi/4$ and (b) α with $\beta = \pi/10$ for NS- $\alpha\beta$.

tions of 64^3 and 128^3 , along with the NS results for a resolution of 256^3 . While all results show good agreement for $k\alpha < 1$, a marked increase in overshoot is evident for NS- $\alpha\beta$ on the finer grid.

We now consider the sensitivity of the energy spectrum to variations in the scales α and β and the resolution. To study flows at slightly higher Reynolds numbers, we increased the magnitude of the forcing in the first two wave-number shells. Figures 3 and 4 show results obtained with resolutions of 64^3 and 128^3 , respectively. The lower resolution (64^3) results were obtained using a normalized kinematic viscosity of $\nu\tau/l^2 = 0.0115$, and resulted in Taylor microscale Reynolds numbers R_λ between 65 and 100. For a given ν and \mathbf{f}_k , de-

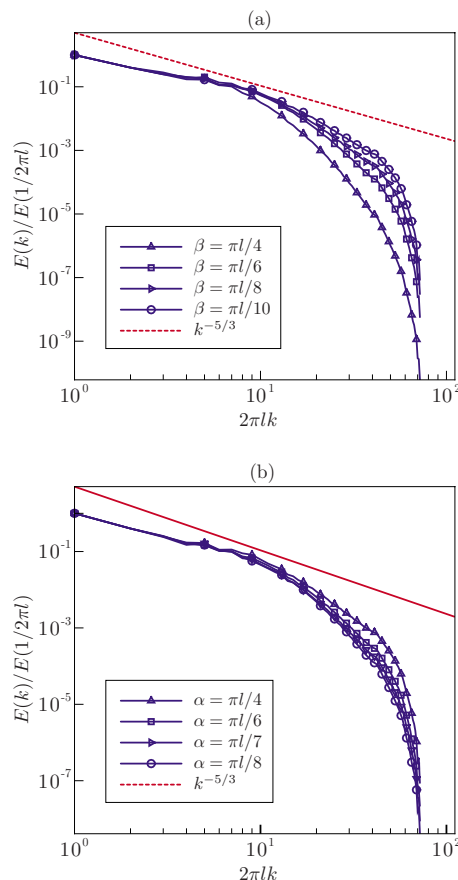


FIG. 4. (Color online) Influence, at 128^3 resolution, of (a) β with $\alpha = \pi/4$ and (b) α with $\beta = \pi/10$ for NS- $\alpha\beta$.

creasing α while holding β fixed increases R_λ . Conversely, decreasing β while holding α fixed decreases R_λ . The finer resolution (128^3) results were obtained using a slightly smaller normalized kinematic viscosity of $\nu\tau/l^2 = 0.0058$, resulting in still larger values of R_λ . Both studies show that, as β is decreased with respect to α , Kolmogorov's $-5/3$ law is better preserved and the decay in the dissipation range becomes steeper. On the other hand, agreement with the $-5/3$ law deteriorates at higher wave numbers and the decay of the energy spectrum in the dissipation range does not become steeper with decreasing α .

Hot-wire anemometry experiments show that the vorticity aligns with the eigenvector corresponding to the intermediate

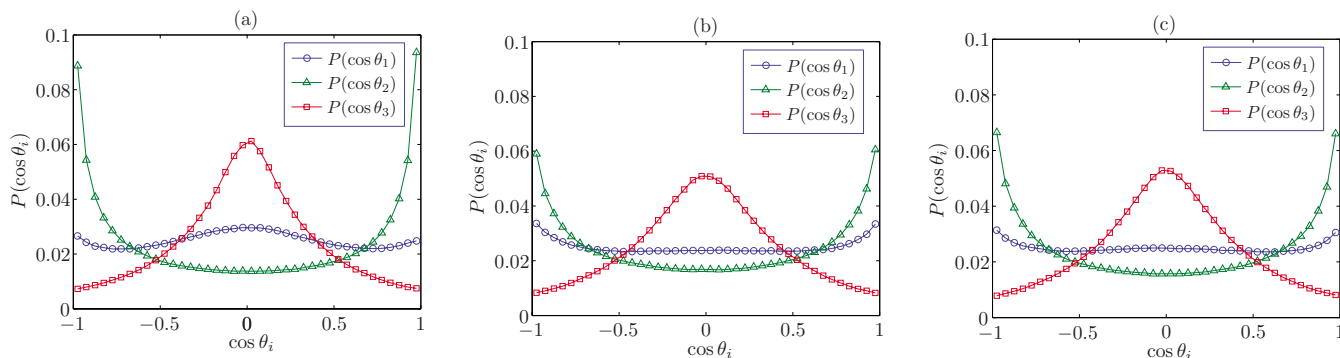


FIG. 5. (Color online) Normalized PDFs $P(\cos \theta_i)$: (a) NS ($\alpha = \beta = 0$) at 256^3 resolution (b) NS- α ($\alpha = \beta = \pi/4$) at 128^3 resolution, (c) NS- $\alpha\beta$ ($\alpha = \pi/4$ and $\beta = \pi/32$) at 128^3 resolution.

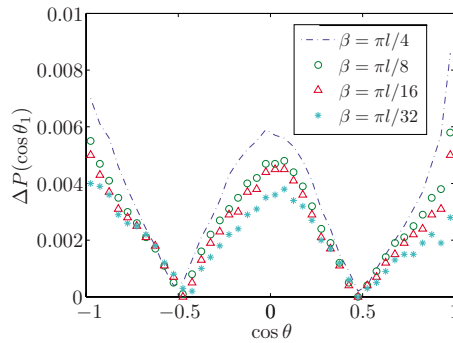


FIG. 6. (Color online) Difference $\Delta P(\cos \theta_1)$, for various values of β , between $P(\cos \theta_1)$ for NS- $\alpha\beta$ (128^3 resolution) and the corresponding normalized PDF for NS (256^3 resolution).

eigenvalue of the stretching tensor [17–19]. Jiménez [20] provided a kinematical explanation for this observation. DNS illustrates the importance of this phenomenon in the formation of sheet-and tube-like structures [21–23]. Let d_i ($i=1,2,3$) denote the eigenvalues of the filtered stretching tensor $\mathbf{D}=\frac{1}{2}[\text{grad } \mathbf{u}+(\text{grad } \mathbf{u})^T]$, ordered according to $d_1 \geq d_2 \geq d_3$, and let \mathbf{e}_i ($i=1,2,3$) denote the corresponding eigenvectors. The angle θ_i between the filtered vorticity $\boldsymbol{\omega}=\text{curl } \mathbf{u}$ and \mathbf{e}_i is given by $\cos \theta_i=\boldsymbol{\omega} \cdot \mathbf{e}_i/|\boldsymbol{\omega}|$. Figure 5 shows the probability density functions (PDFs) $P(\cos \theta_i)$ for the NS, NS- α , and NS- $\alpha\beta$ equations. To compute $P(\cos \theta_i)$ at a given time step, we divided the interval $[-1, 1]$ into subintervals, did histogram counts for each direction cosine, and normalized by the number of grid points. To obtain statistically significant data, the process was performed at numerous time steps after reaching steady state and averages were computed. Plots are provided for $\alpha=\beta=0$ (NS) at 256^3 resolution, $\alpha=\beta=\pi/4$ (NS- α) at 128^3 resolution, and $\alpha=\pi/4$ and $\beta=\pi/32$ (NS- $\alpha\beta$) at 128^3 resolution. The results for NS and NS- α are similar to those obtained by Chen *et al.* [1].

For these results, $P(\cos \theta_1)$ is closer to $P(\cos \theta_3)$ than is the case for the NS equations. As Chen *et al.* [1] noted, this indicates that sheetlike structures predominate over tubelike structures for NS- α . This phenomenon is clearly shown in Fig. 6, which displays the difference $\Delta P(\cos \theta_1)$ between the PDFs of the largest eigenvalues for the NS- $\alpha\beta$ and NS equations, at respective resolutions of 128^3 and 256^3 , for various values of β ; $\Delta P(\cos \theta_1)$ decreases as β decreases, indicating that the vorticity alignment arising from the NS- $\alpha\beta$ equations approaches that arising from the NS equations as β decreases.

This Rapid Communication explores the utility of the recently proposed NS- $\alpha\beta$ equations as a subgrid model for turbulence and the improvements that are available in comparison to the established NS- α equations. Numerical evidence clearly indicates better agreement with the standard NS results for $\beta < \alpha$, consistent with the conjecture of Fried and Gurtin [12]. Appropriate choices of both α and β provide a means to capture both large and intermediate scale features of flows, even at coarser resolutions. The decay of the energy spectrum in the inertial range is mostly affected by α and the extent of the inertial range is mostly affected by β . Numerical results for the PDFs obtained from the filtered vorticity and the eigenvectors of the filtered stretching tensor also indicate better agreement between the NS- $\alpha\beta$ and NS equations as β decreases relative to α . While the results are encouraging, questions remain concerning the optimal choice of β given α and the grid resolution. This is a subject for future work.

The authors are indebted to Professor Shiyi Chen at Johns Hopkins for providing an independent verification of our DNS results and to the Center for Computational Science, Engineering and Medicine at Duke University. Authors Kim, Dolbow, Fried, and Gurtin also acknowledge the partial support of the Department of Energy.

- [1] S. Chen, D. D. Holm, L. G. Margolin, and R. Zhang, *Physica D* **133**, 66 (1999).
- [2] C. Foias, D. D. Holm, and E. S. Titi, *Physica D* **152–153**, 505 (2001).
- [3] J. Pietarila Graham, D. D. Holm, P. Mininni, and A. Pouquet, *Phys. Fluids* **18**, 045106 (2006).
- [4] J. Pietarila Graham, D. D. Holm, P. Mininni, and A. Pouquet, *Phys. Fluids* **20**, 035107 (2008).
- [5] J. Pietarila Graham, D. D. Holm, P. D. Mininni, and A. Pouquet, *Phys. Rev. E* **76**, 056310 (2007).
- [6] S. Chen, C. Foias, D. D. Holm, E. Olson, E. S. Titi, and S. Wynne, *Phys. Rev. Lett.* **81**, 5338 (1998).
- [7] S. Chen, C. Foias, E. Olson, E. S. Titi, and S. Wynne, *Physica D* **133**, 49 (1999).
- [8] S. Chen, C. Foias, E. Olson, E. S. Titi, and S. Wynne, *Phys. Fluids* **11**, 2343 (1999).
- [9] D. D. Holm, J. E. Marsden, and T. Ratiu, *Adv. Math.* **137**, 1 (1998).
- [10] D. D. Holm, J. E. Marsden, and T. Ratiu, *Phys. Rev. Lett.* **80**, 4173 (1998).
- [11] E. Fried and M. E. Gurtin, *Arch. Ration. Mech. Anal.* **182**, 513 (2006).
- [12] E. Fried and M. E. Gurtin, *Phys. Rev. E* **75**, 056306 (2007).
- [13] E. Fried and M. E. Gurtin, *Theor. Comput. Fluid Dyn.* **22**, 433 (2008).
- [14] J. D. Albertson and M. B. Parlange, *Water Resour. Res.* **35**, 2121 (1999).
- [15] J. D. Albertson and M. B. Parlange, *Adv. Water Resour.* **23**, 239 (1999).
- [16] K. Mohseni, B. Kosovic, S. Shkoller, and J. Marsden, *Phys. Fluids* **15**, 524 (2003).
- [17] A. Tsinober, E. Kit, and T. Dracos, *J. Fluid Mech.* **242**, 169 (1992).
- [18] P. Vukoslavcevic and J. M. Wallace, *Meas. Sci. Technol.* **7**, 1451 (1996).
- [19] A. Honkan and Y. Andreopolous, *J. Fluid Mech.* **350**, 29 (1997).
- [20] J. Jiménez, *Phys. Fluids A* **4**, 652 (1992).
- [21] R. Kerr, *J. Fluid Mech.* **153**, 31 (1985).
- [22] Wm. T. Ashurst, A. R. Kerstein, R. M. Kerr, and C. H. Gibson, *Phys. Fluids* **30**, 2343 (1987).
- [23] K. Nomura and G. Post, *J. Fluid Mech.* **377**, 65 (1998).